Simplest, string-derivable, supergravity model and its experimental predictions

Jorge L. Lopez
Center for Theoretical Physics, Department of Physics, Texas A&M University, College Station, Texas 77843-4242 and Astroparticle Physics Group, Houston Advanced Research Center (HARC), The Woodlands, Texas 77381

D. V. Nanopoulos
Center for Theoretical Physics, Department of Physics, Texas A&M University, College Station, Texas 77843-4242 Astroparticle Physics Group, Houston Advanced Research Center (HARC), The Woodlands, Texas 77381 and CERN Theory Division, 1211 Geneva 23, Switzerland

A. Zichichi
CERN, Geneva, Switzerland
(Received 24 June 1993)

We present the simplest, string-derivable, supergravity model and discuss its experimental consequences. This model is a new string-inspired flipped SU(5) which unifies at the string scale $M_U = 10^{18}$ GeV due to the introduction of an additional pair of $\mathbf{10},\overline{\mathbf{10}}$ flipped SU(5) representations which contain new intermediate scale "gap" particles. We study various model-building issues which should be addressed in string-derived incarnations of this model. We focus our study on the no-scale supergravity mechanism and explore thoroughly the three-dimensional parameter space of the model ($m_{\tilde{g}}, m_t, \tan\beta$), thus obtaining several simple relationships among the particle masses, such as $m_{\tilde{q}} \approx m_{\tilde{g}}$, $m_{\tilde{e}_L} \approx m_{\tilde{\nu}} \approx 0.30 m_{\tilde{g}}$, $m_{\tilde{e}_R} \approx 0.18 m_{\tilde{g}}$, and $m_{\chi_2^0} \approx 2m_{\chi_1^0} \approx m_{\chi_1^\pm}$. In a strict interpretation of the no-scale supergravity scenario we solve for $\tan\beta$ as a function of m_t and $m_{\tilde{g}}$, and show that m_t determines not only the sign of the Higgs mixing parameter μ but also whether the lightest Higgs boson mass is above or below 100 GeV. We also find that throughout the parameter space the neutralino relic abundance is within observational bounds ($\Omega_\chi h_0^2 \lesssim 0.25$) and may account for a significant portion of the dark matter in the Universe.

PACS number(s): 04.65.+e, 11.30.Pb, 12.60.Jv, 14.80.Ly

I. INTRODUCTION

The purpose of this paper is to find out the simplest supergravity model compatible with all boundary conditions imposed by present experimental and theoretical knowledge. The first property of this model is the number of parameters needed, which we restrict to a minimum. In this search we follow string-inspired choices. The most significant is the "no-scale" supergravity condition which, in addition to being the only known mechanism to guarantee the existence of light supersymmetric particles, has the very interesting property of being the infrared limit of superstring theory. The other choices, aimed at the minimum number of free parameters, are at present inspired by string phenomenology and are good candidates to being rigorously derivable from string theory. Our main goal is to produce a model whose basic conceptual choices are attractive, in terms of what we think (and hope) will be the final theory of all particles and interactions. One point needs to be emphasized. In order to put string theory under experimental test, the first step is to construct models with a number of parameters, which is as minimal as possible. Our aim is to propose experimental tests that are steps towards the inclusion or exclusion of our choices needed to build the model.

In addition to the very economic grand unified theory (GUT) symmetry-breaking mechanism in flipped SU(5) [1,2], which allows it to be in principle derivable from superstring theory [3], perhaps one of the more interesting motivations for considering such a unified gauge group is the natural avoidance of potentially dangerous dimension-five proton decay operators [4]. In this paper we construct a supergravity model based on this gauge group, which has the additional property of unifying at a scale $M_U \sim 10^{18}$ GeV, as expected to occur in string-derived versions of this model [5]. As such, this model should constitute a blueprint for string model builders. This string unification scale should be contrasted with the naive unification scale, $M_U \sim 10^{16}$ GeV, obtained by running the standard model particles and their superpartners to very high energies. This apparent discrepancy of two orders of magnitude [6] creates a *gap* which needs to be bridged somehow in string models. It has been shown [7] that the simplest solution to this problem is the introduction in the spectrum of heavy vectorlike particles with standard model quantum numbers. The minimal such choice [8], a quark doublet pair $Q,\overline{Q}$ and a 1/3-charge quark singlet pair $D,\overline{D}$, fit snugly inside a $\mathbf{10},\overline{\mathbf{10}}$ pair of flipped SU(5) representations, beyond the usual $3\times(\mathbf{10}+\overline{\mathbf{5}}+\mathbf{1})$ of matter and $\mathbf{10},\overline{\mathbf{10}}$ of Higgs fields.

In this model, gauge symmetry breaking occurs due to vacuum expectation values (VEV's) of the neutral components of the $\mathbf{10},\overline{\mathbf{10}}$ Higgs representations, which devel-

op along flat directions of the scalar potential. There are two known ways in which these VEV's (and thus the symmetry-breaking scale) could be determined:

(i) In the conventional way, radiative corrections to the scalar potential in the presence of soft supersymmetry breaking generate a global minimum of the potential for values of the VEV's slightly below the scale where supersymmetry-breaking effects are first felt in the observable sector [4]. If the latter scale is the Planck scale (in a suitable normalization) then $M_U \sim M_{\rm Pl}/\sqrt{8\pi} \sim 10^{18}$ GeV.

(ii) In string-derived models a pseudo $U_A(1)$ anomaly arises as a consequence of truncating the theory to just the massless degrees of freedom, and adds a contribution to its D term, $D_A = \sum q_i^A |\langle \phi_i \rangle|^2 + \epsilon$, with $\epsilon = g^2 {\rm Tr} U_A(1)/192\pi^2 \sim (10^{18}\ {\rm GeV})^2$ [9]. To avoid a huge breaking of supersymmetry we need to demand $D_A = 0$ and therefore the fields charged under $U_A(1)$ need to get suitable VEV's. Among these one generally finds the symmetry breaking Higgs fields, and thus $M_U \sim 10^{18}$ GeV follows.

In general, both these mechanisms could produce somewhat lower values of M_U. However, $M_U \gtrsim 10^{16}$ GeV is necessary to avoid too rapid proton decay due to dimension-six operators [10]. In these more general cases the SU(5) and U(1) gauge couplings would not unify at M_U (only α_2 and α_3 would), although they would eventually "superunify" at the string scale $M_{\rm SU} \sim 10^{18}$ GeV. To simplify matters, below we consider the simplest possible case of $M_U = M_{\rm SU} \sim 10^{18}$ GeV.

We also draw inspiration from string model building and regard the Higgs mixing term $\mu h \bar{h}$ as a result of an effective higher-order coupling [11], instead of as a result of a light singlet field getting a small VEV (i.e., $\lambda h \bar{h} \phi \to \lambda \langle \phi \rangle h \bar{h}$) as originally considered [2,4].

For the supersymmetry breaking parameters we consider the no-scale ansatz [12], which ensures the vanishing of the (tree-level) cosmological constant even after supersymmetry breaking. This framework also arises in the low-energy limit of superstring theory [13]. In a theory which contains heavy fields, the minimal no-scale structure SU(1,1) [14] is generalized to SU(N,1) [15] which implies that the scalar fields do not feel the supersymmetry breaking effects. In practice this means that the universal scalar mass (m_0) and the universal cubic scalar coupling (A) are set to zero. The sole source of supersymmetry breaking is the universal gaugino mass ($m_{1/2}$). We first let the universal bilinear scalar coupling (B) float, i.e., be determined by the radiative electroweak symmetry breaking constraints. We also consider the strict no-scale scenario where $B(M_U)=0$. It is worth pointing out that with the no-scale framework the value of $m_{1/2}$ should be determined dynamically and explicit calculations [16] show that it should be below 1 TeV. A recent analysis has shown that this result may also occur automatically once all phenomenological constraints on the model have been imposed [17].

We should remark that a real string model will include a hidden sector in addition to the observable sector discussed in what follows. The model presented here tacitly assumes that such hidden sector is present and that it has suitable properties. For example, the superpotential in Eq. (1) below, in a string model will receive contributions from cubic and higher-order terms, with the latter generating effective observable sector couplings once hidden sector matter condensates develop [11]. The hidden sector is also assumed to play a fundamental role in triggering supersymmetry breaking via gaugino condensation. This in turn makes possible the first mechanism for gauge symmetry breaking discussed above. Our comments here are of a generic nature because we do not have a specific string model where these assumptions can be tested explicitly. In the known string models of the class we draw inspiration from (i.e., free fermionic flipped SU(5) models [9]), suitable hidden sectors which do not affect the observable sector Yukawa couplings are known to exist [3,11,21]. Finally, no string model has yet been derived which can accommodate *all* of the phenomenological properties that we know must exist—such an enterprise is clearly beyond the scope of this paper.

This paper is organized as follows. In Sec. II we present the string-inspired model with all the model-building details which determine in principle the masses of the new heavy vectorlike particles. We also discuss the question of the possible reintroduction of dangerous dimension-five proton decay operators in this generalized model. We then impose the constraint of flipped SU(5) unification and string unification to occur at $M_U = 10^{18}$ GeV to deduce the unknown masses. In Sec. III we consider the experimental predictions for all the sparticle and one-loop corrected Higgs boson masses in this model, and deduce several simple relations among the various sparticle masses. In Sec. IV we repeat this analysis for the strict no-scale case. This additional constraint allows us to determine $\tan\beta$ for a given $m_{\tilde{g}}$ and m_t (up to a possible twofold ambiguity), and thus to sharpen the most $\tan\beta$-sensitive predictions. In Sec. V we summarize our conclusions.

II. THE MODEL

The model we consider is a generalization of that presented in Ref. [2], and contains the following flipped SU(5) fields: (i) three generations of quark and lepton fields $F_i, \bar{f}_i, l_i^c$, $i = 1,2,3$; (ii) two pairs of Higgs $\mathbf{10}, \overline{\mathbf{10}}$ representations $H_i, \bar{H}_i$, $i = 1,2$; (iii) one pair of "electroweak" Higgs $\mathbf{5}, \overline{\mathbf{5}}$ representations $h, \bar{h}$; (iv) three singlet fields $\phi_{1,2,3}$.

Under SU(3)×SU(2) the various flipped SU(5) fields decompose as follows:

$$F_i = \{Q_i, d_i^c, \nu_i^c\}\ ,\quad \bar{f}_i = \{L_i, u_i^c\}\ ,\quad l_i^c = e_i^c\ , \tag{2.1a}$$

$$H_i = \{Q_{H_i}, d_{H_i}^c, \nu_{H_i}^c\}\ ,\quad \bar{H}_i = \{Q_{\bar{H}_i}, d_{\bar{H}_i}^c, \nu_{\bar{H}_i}^c\}\ , \tag{2.1b}$$

$$h = \{H, D\}\ ,\quad \bar{h} = \{\bar{H}, \bar{D}\}\ . \tag{2.1c}$$

The most general effective[1] superpotential consistent with $SU(5)\times U(1)$ symmetry is given by

$$W=\lambda_1^{ij}F_iF_jh+\lambda_2^{ij}F_i\bar{f}_j\bar{h}+\lambda_3^{ij}\bar{f}_il_j^ch+\mu h\bar{h}+\lambda_4^{ij}H_iH_jh$$
$$+\lambda_5^{ij}\bar{H}_i\bar{H}_j\bar{h}+\lambda_{1'}^{ij}H_iF_jh+\lambda_{2'}^{ij}H_i\bar{f}_j\bar{h}$$
$$+\lambda_6^{ijk}F_i\bar{H}_j\phi_k+w^{ij}H_i\bar{H}_j+\mu^{ij}\phi_i\phi_j\ . \tag{2.2}$$

Symmetry breaking is effected by nonzero VEV's $\langle\nu_{H_i}^c\rangle=V_i$, $\langle\nu_{\bar{H}_i}^c\rangle=\bar{V}_i$, such that $V_1^2+V_2^2=\bar{V}_1^2+\bar{V}_2^2$.

A. Higgs doublet and triplet mass matrices

The Higgs doublet mass matrix receives contributions from $\mu h\bar{h}\to\mu H\bar{H}$ and $\lambda_{2'}^{ij}H_i\bar{f}_j\bar{h}\to\lambda_{2'}^{ij}V_iL_j\bar{H}$. The resulting matrix is

$$\mathcal{M}_2=\begin{array}{c} \\ H \\ L_1 \\ L_2 \\ L_3 \end{array}\begin{array}{c} \begin{array}{c}\bar{H}\end{array} \\ \begin{pmatrix}\mu\\ \lambda_{2'}^{i1}V_i\\ \lambda_{2'}^{i2}V_i\\ \lambda_{2'}^{i3}V_i\end{pmatrix}\end{array}. \tag{2.3}$$

To avoid fine tunings of the $\lambda_{2'}^{ij}$ couplings we must demand $\lambda_{2'}^{ij}\equiv 0$, so that $\bar{H}$ remains light.

The Higgs triplet matrix receives several contributions: $\mu h\bar{h}\to\mu D\bar{D}$; $\lambda_{1'}^{ij}H_iF_jh\to\lambda_{1'}^{ij}V_id_j^cD$; $\lambda_4^{ij}H_iH_jh\to\lambda_4^{ij}V_id_{H_j}^cD$; $\lambda_5^{ij}\bar{H}_i\bar{H}_j\bar{h}\to\lambda_5^{ij}\bar{V}_id_{\bar{H}_j}^c\bar{D}$; $w^{ij}d_{H_i}^cd_{\bar{H}_j}^c$. The resulting matrix is[2]

$$\mathcal{M}_3=\begin{array}{c} \\ D \\ d_{\bar{H}_1}^c \\ d_{\bar{H}_2}^c \end{array}\begin{array}{c} \begin{array}{cccccc}\bar{D} & d_{H_1}^c & d_{H_2}^c & d_1^c & d_2^c & d_3^c\end{array} \\ \begin{pmatrix}\mu & \lambda_4^{i1}V_i & \lambda_4^{i2}V_i & \lambda_{1'}^{i1}V_i & \lambda_{1'}^{i2}V_i & \lambda_{1'}^{i3}V_i\\ \lambda_5^{i1}\bar{V}_i & w_{11} & w_{12} & 0 & 0 & 0\\ \lambda_5^{i2}\bar{V}_i & w_{21} & w_{22} & 0 & 0 & 0\end{pmatrix}\end{array}. \tag{2.4}$$

Clearly three linear combinations of $\{\bar{D},d_{H_{1,2}}^c,d_{1,2,3}^c\}$ will remain light. In fact, such a general situation will induce a mixing in the down-type Yukawa matrix $\lambda_1^{ij}F_iF_jh\to\lambda_1^{ij}Q_id_j^cH$, since the d_j^c will need to be reexpressed in terms of these mixed light eigenstates.[3] This low-energy quark-mixing mechanism is an explicit realization of the general extra-vector-abeyance (EVA) mechanism of Ref. [19]. As a first approximation though, in what follows we will set $\lambda_{1'}^{ij}=0$, so that the light eigenstates are $d_{1,2,3}^c$.

B. Neutrino seesaw matrix

The seesaw neutrino matrix receives contributions from $\lambda_2^{ij}F_i\bar{f}_j\bar{h}\to m_u^{ij}\nu_i^c\nu_j$, $\lambda_6^{ijk}F_i\bar{H}_j\phi_k\to\lambda_6^{ijk}\bar{V}_j\nu_i^c\phi_k$, $\mu^{ij}\phi_i\phi_j$. The resulting matrix is[4]

$$\mathcal{M}_\nu=\begin{array}{c} \\ \nu_i \\ \nu_i^c \\ \phi_i \end{array}\begin{array}{c} \begin{array}{ccc}\nu_j & \nu_j^c & \phi_j\end{array} \\ \begin{pmatrix}0 & m_u^{ji} & 0\\ m_u^{ij} & 0 & \lambda_6^{ikj}\bar{V}_k\\ 0 & \lambda_6^{jki}\bar{V}_k & \mu^{ij}\end{pmatrix}\end{array}. \tag{2.5}$$

C. Numerical scenario

To simplify the discussion we will assume, besides[5] $\lambda_{1'}^{ij}=\lambda_{2'}^{ij}\equiv 0$, that

$$\lambda_4^{ij}=\delta^{ij}\lambda_4^{(i)},\quad \lambda_5^{ij}=\delta^{ij}\lambda_5^{(i)},\quad \lambda_6^{ijk}=\delta^{ij}\delta^{ik}\lambda_6^{(i)}\ ,$$
$$\mu^{ij}=\delta^{ij}\mu_i,\quad w^{ij}=\delta^{ij}w_i\ . \tag{2.6}$$

These choices are likely to be realized in string versions of this model and will not alter our conclusions below. In this case the Higgs triplet mass matrix reduces to

$$\mathcal{M}_3=\begin{array}{c} \\ D \\ d_{\bar{H}_1}^c \\ d_{\bar{H}_2}^c \end{array}\begin{array}{c} \begin{array}{ccc}\bar{D} & d_{H_1}^c & d_{H_2}^c\end{array} \\ \begin{pmatrix}\mu & \lambda_4^{(1)}V_1 & \lambda_4^{(2)}V_2\\ \lambda_5^{(1)}\bar{V}_1 & w_1 & 0\\ \lambda_5^{(2)}\bar{V}_2 & 0 & w_2\end{pmatrix}\end{array}. \tag{2.7}$$

Regarding the (3,2) states, the scalars get either eaten by the X,Y SU(5) heavy gauge bosons or become heavy Higgs bosons, whereas the fermions interact with the $\tilde{X},\tilde{Y}$ gauginos through the mass matrix [21]

$$\mathcal{M}_{(3,2)}=\begin{array}{c} \\ Q_{H_1} \\ Q_{H_2} \\ \tilde{X} \end{array}\begin{array}{c} \begin{array}{ccc}Q_{\bar{H}_1} & Q_{\bar{H}_2} & \tilde{Y}\end{array} \\ \begin{pmatrix}w_1 & 0 & g_5V_1\\ 0 & w_2 & g_5V_2\\ g_5\bar{V}_1 & g_5\bar{V}_2 & 0\end{pmatrix}\end{array}. \tag{2.8}$$

---

[1]To be understood in the string context as arising from cubic and higher order terms [18,11].

[2]The zero entries in $\mathcal{M}_3$ result from the assumption $\langle\phi_k\rangle=0$ in $\lambda_6^{ijk}F_i\bar{H}_j\phi_k$.

[3]Note that this mixing is on top of any structure that λ_1^{ij} may have, and is the only source of mixing in the typical string model-building case of a diagonal λ_2 matrix.

[4]We neglect a possible higher-order contribution which could produce a nonvanishing $\nu_i^c\nu_j^c$ entry [20].

[5]In Ref. [2] the discrete symmetry $H_1\to -H_1$ was imposed so that these couplings automatically vanish when $H_2,\bar{H}_2$ are not present. This symmetry (generalized to $H_i\to -H_i$) is not needed here since it would imply $w^{ij}\equiv 0$, which is shown below to be disastrous for gauge coupling unification.

The lightest eigenvalues of these two matrices (denoted generally by d_H^c and Q_H, respectively) constitute the new relatively light particles in the spectrum, which are hereafter referred to as the "*gap*" particles since with suitable masses they bridge the gap between unification masses at 10^{16} and 10^{18} GeV.

Guided by the phenomenological requirement on the gap particle masses, i.e., $M_{Q_H} \gg M_{d_H^c}$ [8], we consider the explicit numerical scenario

$$\lambda_4^{(2)}=\lambda_5^{(2)}=0\ ,\quad V_1,\bar{V}_1,V_2,\bar{V}_2 \sim V \gg w_1 \gg w_2 \gg \mu\ , \tag{2.9}$$

which would need to be reproduced in a viable string-derived model. From Eq. (2.7) we then get $M_{d_{H_2}^c}=M_{d_{\bar{H}_2}^c}=w_2$, and all other mass eigenstates $\sim V$. Furthermore, $\mathcal{M}_{(3,2)}$ has a characteristic polynomial $\lambda^3-\lambda^2(w_1+w_2)-\lambda(2V^2-w_1w_2)+(w_1+w_2)V^2=0$, which has two roots of $O(V)$ and one root of $O(w_1)$. The latter corresponds to $\sim(Q_{H_1}-Q_{H_2})$ and $\sim(Q_{\bar{H}_1}-Q_{\bar{H}_2})$. In sum then, the gap particles have masses $M_{Q_H}\sim w_1$ and $M_{d_H^c}\sim w_2$, whereas all other heavy particles have masses $\sim V$.

The see-saw matrix reduces to

$$\mathcal{M}_\nu = \begin{array}{c} \\ \nu_i \\ \nu_i^c \\ \phi_i \end{array} \begin{array}{c} \begin{array}{ccc} \nu_i & \nu_i^c & \phi_i \end{array} \\ \begin{pmatrix} 0 & m_u^i & 0 \\ m_u^i & 0 & \lambda_6^{(i)}\bar{V}_i \\ 0 & \lambda_6^{(i)}\bar{V}_i & \mu^i \end{pmatrix} \end{array}, \tag{2.10}$$

for each generation. The physics of this see-saw matrix has been discussed recently in Ref. [20], where it was shown to lead to an interesting amount of hot dark matter (ν_τ) and a Mikheyev-Smirnov-Wolfenstein (MSW) effect (ν_e,ν_μ) compatible with all solar neutrino data.

D. Proton decay

The dimension-six operators mediating proton decay in this model are highly suppressed due to the large mass of the X,Y gauge bosons ($\sim M_U=10^{18}$ GeV). Higgsino mediated dimension-five operators exist and are naturally suppressed in the minimal model of Ref. [2]. The reason for this is that the Higgs triplet mixing term $\mu h\bar{h}\to\mu D\bar{D}$ is small ($\mu\sim M_Z$), whereas the Higgs triplet mass eigenstates obtained from Eq. (2.4) by just keeping the 2×2 submatrix in the upper left-hand corner, are always very heavy ($\sim V$). The dimension-five mediated operators are then proportional to μ/V^2 and thus the rate is suppressed by a factor or $(\mu/V)^2\ll1$ relative to the unsuppressed case found in the standard SU(5) model.

In the generalized model presented here, the Higgs triplet mixing term is still $\mu D\bar{D}$. However, the exchanged mass eigenstates are not necessarily all very heavy. In fact, above we have demanded the existence of a relatively light ($\sim w_1$) Higgs triplet state (d_H^c). In this case the operators are proportional to $\mu\alpha_i\bar{\alpha}_i/\mathcal{M}_i^2$, where $\mathcal{M}_i$ is the mass of the ith exchanged eigenstate and α_i, $\bar{\alpha}_i$ are its $D,\bar{D}$ admixtures. In the scenario described above, the relatively light eigenstates ($d_{H_2}^c,d_{\bar{H}_2}^c$) contain no $D,\bar{D}$ admixtures, and the operator will again be $\propto\mu/V^2$.

TABLE I. The value of the gap particle masses and the unified coupling for $\alpha_3(M_Z)=0.118\pm0.008$. We have taken $M_U=10^{18}$ GeV, $\sin^2\theta_W=0.233$, and $\alpha_e^{-1}=127.9$.

$\alpha_3(M_Z)$	$M_{d_H^c}$ (GeV)	M_{Q_H} (GeV)	$\alpha(M_U)$
0.110	4.9×10^4	2.2×10^{12}	0.0565
0.118	4.5×10^6	4.1×10^{12}	0.0555
0.126	2.3×10^8	7.3×10^{12}	0.0547

Note, however, that if conditions (2.9) (or some analogous suitability requirement) are not satisfied, then diagonalization of $\mathcal{M}_3$ in Eq. (2.7) may reintroduce a sizable dimension-five mediated proton decay rate, depending on the value of the $\alpha_i,\bar{\alpha}_i$ coefficients. To be safe one should demand [22,23]

$$\frac{\mu\alpha_i\bar{\alpha}_i}{\mathcal{M}_i^2} \lesssim \frac{1}{10^{17}\ \text{GeV}}\ . \tag{2.11}$$

For the higher values of $M_{d_H^c}$ in Table I (see below), this constraint can be satisfied for not necessarily small values of $\alpha_i,\bar{\alpha}_i$.

E. Gauge coupling unification

Since we have chosen $V\sim M_U=M_{\rm SU}=10^{18}$ GeV, this means that the standard model gauge couplings should unify at the scale M_U. However, their running will be modified due to the presence of the gap particles. Note that the underlying flipped SU(5) symmetry, even though not evident in this respect, is nevertheless essential in the above discussion. The masses M_Q and $M_{d_H^c}$ can then be determined as [8]

$$\ln\frac{M_{Q_H}}{m_Z}=\pi\left(\frac{1}{2\alpha_e}-\frac{1}{3\alpha_3}-\frac{\sin^2\theta_W-0.0029}{\alpha_e}\right) -2\ln\frac{M_U}{m_Z}-0.63\ , \tag{2.12a}$$

$$\ln\frac{M_{d_H^c}}{m_Z}=\pi\left(\frac{1}{2\alpha_e}-\frac{7}{3\alpha_3}+\frac{\sin^2\theta_W-0.0029}{\alpha_e}\right) -6\ln\frac{M_U}{m_Z}-1.47\ , \tag{2.12b}$$

where α_e, α_3, and $\sin^2\theta_W$ are all measured at M_Z. This is a one-loop determination (the constants account for the dominant two-loop corrections) which neglects all low- and high-energy threshold effects,[6] but is quite adequate

[6]Here we assume a common supersymmetric threshold at M_Z. In fact, the supersymmetric threshold and the d_H^c mass are anticorrelated. See Ref. [8] for a discussion.

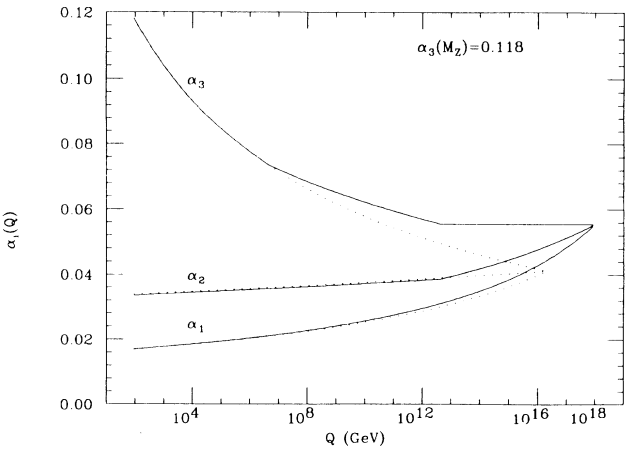

FIG. 1. The running of the gauge couplings in the flipped SU(5) model for $\alpha_3(M_Z)=0.118$ (solid lines). The gap particle masses have been derived using the gauge coupling renormalization group equations to achieve unification at $M_U=10^{18}$ GeV. The case with no gap particles (dotted lines) is also shown; here $M_U\approx 10^{16}$ GeV.

for our present purposes. As shown in Table I [and formula (2.12b)] the d_H^c mass depends most sensitively on $\alpha_3(M_Z)=0.118\pm 0.008$ [24], whereas the Q_H mass and the unified coupling are rather insensitive to it. The unification of the gauge couplings is shown in Fig. 1 (solid lines) for the central value of $\alpha_3(M_Z)$. This figure also shows the case of no gap particles (dotted lines), for which $M_U\approx 10^{16}$ GeV.

III. EXPERIMENTAL PREDICTIONS

The model presented in the previous section can be analyzed to determine its low-energy experimental predictions for e.g., the Higgs and sparticle masses. Consistent with the assumption of flipped SU(5) gauge symmetry breaking at $\sim M_U=10^{18}$ GeV, we assume that the onset of universal supersymmetry breaking in the observable sector occurs at this same scale [4]. This can be parametrized in terms of a universal gaugino mass ($m_{1/2}$), a universal scalar mass (m_0), and universal trilinear (A) and bilinear (B) scalar couplings. One also needs to specify the fermion Yukawa couplings and the Higgs mixing parameter μ. The renormalization group equations then run the relevant parameters to low energies where radiative electroweak symmetry breaking occurs (studied using the one-loop effective potential). When all is said and done, the whole theory can be specified in terms of just five parameters: $m_{1/2}, m_0, A$, the ratio of Higgs vacuum expectation values $\tan\beta$, and the top-quark mass m_t. Note that in this scheme μ and B are calculated quantities; the sign of μ remains undetermined. Our calculations enforce all known experimental bounds on supersymmetric and one-loop corrected Higgs boson masses. We refer the reader to Ref. [25] for a detailed account of this procedure. As discussed in the Introduction, in what follows we consider the typical no-scale supergravity boundary conditions [12], where $m_0=A=0$.[7] In this section we let B float and in the following section we consider the strict no-scale case where $B(M_U)=0$ is required.

For each sign of μ we have explored a three-dimensional grid in this parameter space: $\tan\beta=2-50(2)$, $m_{1/2}=50-500(6)$ GeV, $m_t=95-195(5)$ GeV, where the numbers in parentheses indicate the size of the step taken in that particular direction. Larger values of $\tan\beta$ and/or m_t violate perturbative unification, and $m_{1/2}>500$ GeV leads to $m_{\tilde q}, m_{\tilde g}>1$ TeV, which would make the theory "unnatural." As discussed in the Introduction, the correct superstring model will have to provide an explanation for why these masses are light, and if not so, why this is not unnatural. For now we just take this to be true realizing that relaxing this assumption will not add regions for parameter space which could be tested experimentally at the next generation of colliders. On the other hand, at least in the realm of supergravity, the condition $m_{\tilde q}, m_{\tilde g}<1$ TeV is granted by the no-scale supergravity mechanism [16] and we believe that the correct superstring model will reproduce this important condition. Our exploration resulted in ≈ 12 K acceptable points for each sign of μ, and for all of these we found

$$\tan\beta\lesssim 32 \text{ and } m_t\lesssim 185 \text{ GeV} . \tag{3.1}$$

A. Mass ranges

The restriction of $m_{\tilde q}, m_{\tilde g}<1$ TeV cuts off the growth of most of the sparticle and Higgs boson masses at ≈ 1 TeV. However, the sleptons, the lightest Higgs boson, the two lightest neutralinos, and the lightest chargino are cut off at a much lower mass, as follows[8]:

$$\begin{aligned} &m_{\tilde e_R}<190 \text{ GeV} , \quad m_{\tilde e_L}<305 \text{ GeV} , \quad m_{\tilde\nu}<295 \text{ GeV} , \\ &m_{\tilde\tau_1}<185 \text{ GeV} , \quad m_{\tilde\tau_2}<315 \text{ GeV} , \quad m_h<135 \text{ GeV} , \\ &m_{\chi_1^0}<145 \text{ GeV} , \quad m_{\chi_2^0}<285 \text{ GeV} , \quad m_{\chi_1^\pm}<285 \text{ GeV} . \end{aligned} \tag{3.2}$$

It is interesting to note that due to the various constraints on the model, the gluino and squark masses are predicted to satisfy the current experimental bounds automatically. We find $m_{\tilde g}\gtrsim 220$ GeV and $m_{\tilde q}\gtrsim 200$ GeV, except for the lightest stop eigenstate $\tilde t_1$, which can be as light as ≈ 150 GeV. Therefore, the $\tilde t_1$ squark could be the first squark to be possibly observed at Fermilab in the near future.

---

[7] In Refs. [17,25] a similar analysis was performed for a model without the gap particles (i.e., where $M_U\sim 10^{16}$ GeV). In Ref. [25] an SU(3)×SU(2)×U(1) version of the model presented in this paper was considered (referred to as the SISM model), although only a rather limited analysis was performed.

[8] In this class of supergravity models the three sneutrinos ($\tilde\nu$) are degenerate in mass. Also, $m_{\tilde\mu_L}=m_{\tilde e_L}$ and $m_{\tilde\mu_R}=m_{\tilde e_R}$.

TABLE II. The value of the c_i coefficients appearing in Eq. (3.3) for $\alpha_3(M_Z)=0.118\pm0.008$. Also shown is the ratio $c_{\tilde{g}}=m_{\tilde{g}}/m_{1/2}$.

i	c_i (0.110)	c_i (0.118)	c_i (0.126)
$\tilde{u}_L,\tilde{d}_L$	3.98	4.41	4.97
$\tilde{u}_R$	3.68	4.11	4.66
$\tilde{d}_R$	3.63	4.06	4.61
$\tilde{\nu},\tilde{e}_L$	0.406	0.409	0.413
$\tilde{e}_R$	0.153	0.153	0.153
$c_{\tilde{g}}$	1.95	2.12	2.30

B. Mass relations

The first and second generation squark and slepton masses can be determined analytically:

$$\tilde{m}_i^2=m_{1/2}^2(c_i+\xi_0^2)-d_i\frac{\tan^2\beta-1}{\tan^2\beta+1}M_W^2 , \tag{3.3}$$

where $d_i=(T_{3i}-Q)\tan^2\theta_W+T_{3i}$ (e.g., $d_{\tilde{u}_L}=\frac{1}{2}-\frac{1}{6}\tan^2\theta_W$, $d_{\tilde{e}_R}=-\tan^2\theta_W$), and in our case $\xi_0=m_0/m_{1/2}=0$. The coefficients c_i can be calculated numerically in terms of the low-energy gauge couplings, and are given in Table II[9] for $\alpha_3(M_Z)=0.118\pm0.008$. In the table it is also shown $c_{\tilde{g}}=m_{\tilde{g}}/m_{1/2}$. The "average" squark mass $m_{\tilde{q}}\equiv\frac{1}{8}(m_{\tilde{u}_L}+m_{\tilde{u}_R}+m_{\tilde{d}_L}+m_{\tilde{d}_R}+m_{\tilde{c}_L}+m_{\tilde{c}_R}+m_{\tilde{s}_L}+m_{\tilde{s}_R})$ is then determined to be

$$m_{\tilde{q}}=0.97m_{\tilde{g}} , \tag{3.4}$$

within $\pm3\%$, allowing for a $\pm1\sigma$ error in $\alpha_3(M_Z)$ (the dependence on $\tan\beta$ is negligible). The squark splitting around the average is $\approx2\%$.

The third-generation squarks deviate considerably from the average squark mass and have a non-negligible dependence on $\tan\beta$ due to the off-diagonal elements on the squark mass matrix (which are proportional to the corresponding quark mass). Throughout the parameter space we found the following maximal relative deviations of these squark masses relative to the average squark mass (i.e., $|m_{\tilde{q}_i}-m_{\tilde{q}}|/m_{\tilde{q}}$):

$$\tilde{b}_1:\lesssim14\% \ ; \quad \tilde{b}_2:\lesssim8\% \ ; \quad \tilde{t}_1:\lesssim47\% \ ; \quad \tilde{t}_2:\lesssim35\% . \tag{3.5}$$

In Fig. 2 we plot[10] the bottom-squark and top-squark masses. The bottom-squark masses are not split enough so that $m_{\tilde{b}_1}$ and $m_{\tilde{b}_2}$ blend into a wide band. The top-squark masses are separated in the figure. Note the lesser definition of the $\tilde{t}_1$ masses due to the relatively larger m_t and $\tan\beta$ effects. For all these masses one should note that the average squark mass $m_{\tilde{q}}=0.97m_{\tilde{g}}$ runs somewhere in between these mass bands.

The sleptons are much lighter than the squarks since roughly $m_{\tilde{l}}/m_{\tilde{q}}\approx(c_{\tilde{l}}/c_{\tilde{q}})^{1/2}\lesssim0.3$. In principle, for small $m_{\tilde{g}}$, one would expect a stronger $\tan\beta$ dependence for sleptons due to the relatively smaller contribution of the first term in Eq. (3.3). This, together with the large difference between $c_{\tilde{\nu},\tilde{e}_L}$ and $c_{\tilde{e}_R}$, implies that an "average" slepton mass [as usually assumed in phenomenological studies of the minimal supersymmetric standard model (MSSM)] is a rather *poor* approximation to this model. In Fig. 3 we show the $\tilde{\tau}_{1,2}$ and $\tilde{e}_{L,R}$ masses; the inadequacy of the average slepton mass approximation is evident. As expected, the off-diagonal elements in the $\tilde{\tau}$ mass matrix give a broad band of $\tilde{\tau}_{1,2}$ masses for a given $m_{\tilde{g}}$ value. On the other hand, the $\tilde{e}_{L,R}$ masses look much sharper as a function of $m_{\tilde{g}}$. What happens is that for small $m_{\tilde{g}}$, when the $\tan\beta$ effects are potentially important, $\tan\beta$ is not allowed to become large and thus the D term is suppressed. The $\tilde{\nu}$ masses start off below $m_{\tilde{e}_R}$ and quickly approach the $m_{\tilde{e}_L}$ line. In numbers we find

$$m_{\tilde{e}_L}\approx m_{\tilde{\nu}}\approx0.302m_{\tilde{g}} \ , \quad m_{\tilde{e}_R}\approx0.185m_{\tilde{g}} , \tag{3.6}$$

where the small D-term contribution has been neglected; it becomes negligible for increasingly larger values of $m_{\tilde{g}}$. The $\tilde{\tau}_1$ ($\tilde{\tau}_2$) mass approximates $\tilde{e}_R$ ($\tilde{e}_L,\tilde{\nu}$) as a "central value," but has quite a spread around it, as Fig. 3 shows.

We find that throughout the parameter space $|\mu|$ is generally much larger than M_W and $|\mu|>M_2$. This is shown on the top row of Fig. 4. Note that $|\mu|\propto m_{\tilde{g}}$ with the $\tan\beta$-dependent slope growing with the value of m_t [25]; the three values of m_t used are evident in the figure. This behavior points to a simple eigenvalue structure for the two lightest neutralinos and the lightest chargino [26]:

$$m_{\chi_1^0}\approx\tfrac{1}{2}m_{\chi_2^0} \ ; \quad m_{\chi_2^0}\approx m_{\chi_1^\pm}\approx M_2=\alpha_2/\alpha_3 m_{\tilde{g}}\approx0.3m_{\tilde{g}} . \tag{3.7}$$

In practice we find $m_{\chi_2^0}\approx m_{\chi_1^\pm}$ to be satisfied quite accurately (see Fig. 5, top row), whereas $m_{\chi_1^0}\approx\frac{1}{2}m_{\chi_2^0}$ is only qualitatively satisfied (see Fig. 5, bottom row). In fact, these two mass relations are much more reliable than the one that links them to $m_{\tilde{g}}$ (not shown). The heavier neutralino ($\chi_{3,4}^0$) and chargino ($\chi_2^\pm$) masses are determined by the value of $|\mu|$ (shown in Fig. 4); they all approach this limit for large enough $|\mu|$. More precisely, $m_{\chi_3^0}$ approaches $|\mu|$ sooner than $m_{\chi_4^0}$ does. On the other hand, $m_{\chi_4^0}$ approaches $m_{\chi_2^\pm}$ rather quickly.

The one-loop corrected lightest Higgs boson mass (m_h) is shown in Fig. 6 (top row). The three noticeable bands

[9]These are renormalized at the scale M_Z. In a more accurate treatment, the c_i would be renormalized at the physical sparticle mass scale, leading to second-order shifts on the sparticle masses.

[10]For all the scatter plots shown in this paper we have restricted the values of the top-quark mass to $m_t=100$, 130, and 160 GeV to have a manageable number of points.

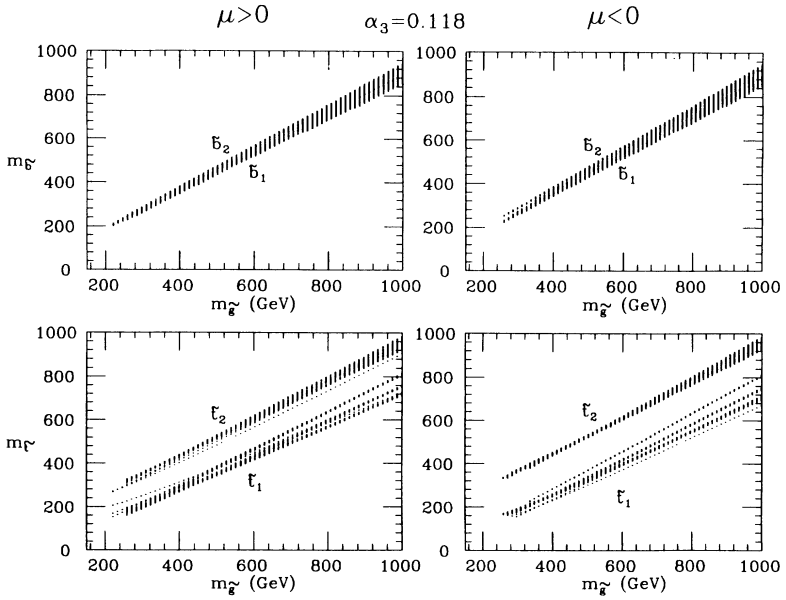

FIG. 2. Scatter plots of the bottom-squark ($\tilde{b}_{1,2}$) and the top-squark ($\tilde{t}_{1,2}$) mass eigenstates vs $m_{\tilde{g}}$. (The $\tilde{b}_{1,2}$ cannot be resolved in this manner.) The average squark mass (first two generations) is $m_{\tilde{q}} \approx 0.97 m_{\tilde{g}}$. From this figure onward, all results are shown for both signs of μ.

correspond to the three values of the top-quark mass used ($m_t = 100$, 130, 160 GeV), for large values of tanβ. For smaller values of tanβ the tree-level contribution is suppressed and the curves reach down to low values of m_h. In this case one can most easily note the expected logarithmic rise of m_h with the squark mass (recall that $m_{\tilde{q}} \approx m_{\tilde{g}}$). For low m_t the curves rise very slightly. However, for large m_t these rise quite dramatically. This is all in agreement with the expected behavior deduced from the approximate analytical expressions for m_h in the literature. In the figure ($m_t \leq 160$ GeV) we get $m_h \lesssim 120$ GeV. Allowing for the whole range of m_t values this upper bound gets relaxed to ≈ 135 GeV. The one-loop corrected pseudoscalar mass m_A is also shown in Fig. 6 as a function of m_h. The three bands correspond to from-left-to-right $m_t = 100$, 130, 160 GeV. The predictions for m_A are not very sharp. It is nevertheless true that for all points examined $m_A > m_h$, as expected from general considerations [27]. The other two Higgs boson states H and H^+ are approached from below by m_A [28]. For $m_{H,H^+} \gtrsim 200$ (300) GeV the difference is $\lesssim 8\%$ (3%).

To appreciate the relations among the sparticle masses in this model, in Fig. 7 we show a graphical display of the spectrum for $m_{\tilde{g}} = 300$ GeV and $m_t = 130$ GeV and both signs of μ. The masses generally scale with $m_{\tilde{g}}$. The masses shown are also given in Table III where in addi-

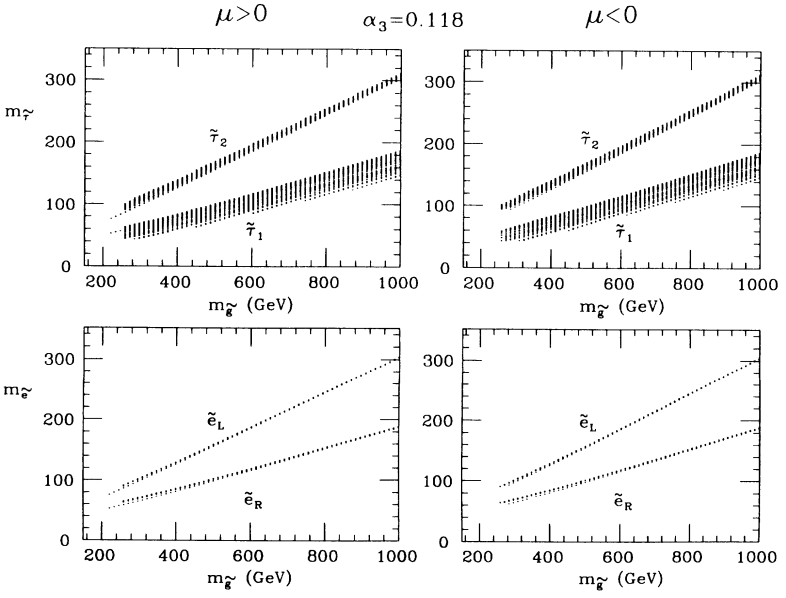

FIG. 3. Scatter plots for the stau ($\tilde{\tau}_{1,2}$) and selectron (or smuon) ($\tilde{e}_{L,R}$) masses. Note the spread in the $\tilde{\tau}_{1,2}$ masses for fixed $m_{\tilde{g}}$, due to the off-diagonal entries in the stau mass matrix. The $\tilde{\nu}$ mass (not shown) starts off slightly below the $\tilde{e}_R$ mass and then quickly joins the $\tilde{e}_L$ line.

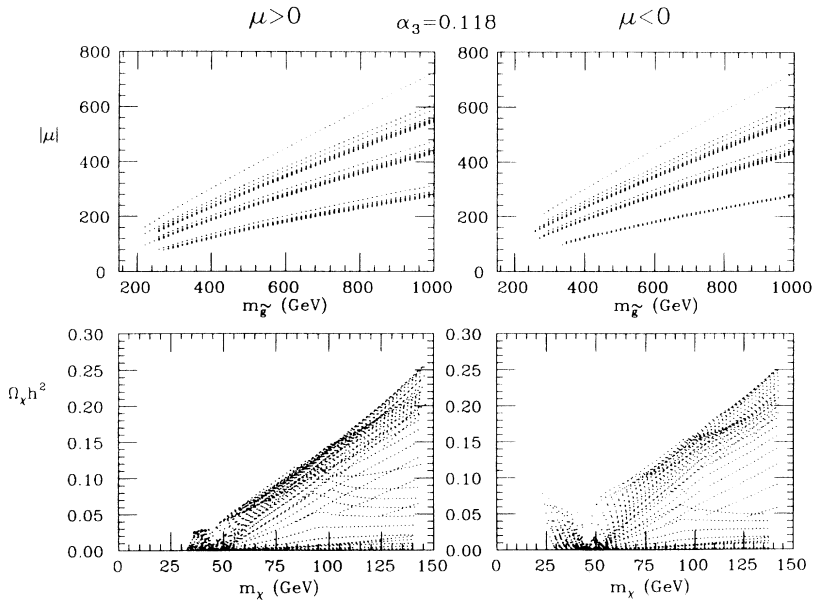

FIG. 4. Scatter plots of the Higgs mixing term (μ) vs $m_{\tilde{g}}$ and the neutralino cosmic relic abundance ($\Omega_\chi h_0^2$) vs m_χ. Note the proportionality $|\mu| \propto m_{\tilde{g}}$ whose slope increases with m_t ($m_t = 100$, 130, and 160 GeV shown). Also, for $m_\chi \approx \frac{1}{2} M_Z$, the Z-pole annihilation is quite noticeable.

tion we give the percentage deviations of the masses relative to their central values due to the variation of $\tan\beta$ over all its allowed range ($2 \lesssim \tan\beta \lesssim 32$).

C. Neutralino dark matter

In Fig. 4 (bottom row) we plot the result for the cosmic relic abundance of the lightest neutralino, $\Omega_\chi h_0^2$. This has been calculated following the methods of Refs. [29]. Since $m_\chi \equiv m_{\chi_1^0}$ grows with $m_{\tilde{g}}$, and $|\mu|$ grows with $m_{\tilde{g}}$, then as m_χ grows, the pure gaugino region ($|\mu| \gg M_2 \approx 0.3 m_{\tilde{g}}$) is approached and the neutralino pair-annihilation is suppressed, leading to larger $\Omega_\chi h_0^2$ values. Note the effect of the Z pole for $m_\chi \approx \frac{1}{2} M_Z$. We find that $\Omega_\chi h_0^2$ can be as large as ≈ 0.25. This result is in good agreement with the observational upper bound on $\Omega_\chi h_0^2$ [30] and does not constrain the model any further. Moreover, fits to the Cosmic Background Explorer (COBE) data and the small and large scale structure of the Universe suggest [31] a mixture of $\approx 70\%$ cold dark matter and $\approx 30\%$ hot dark matter together with $h_0 \approx 0.5$. The hot dark matter component in the form of massive τ neutrinos has already been shown to be compatible with the flipped SU(5) model we consider here [20], whereas the cold dark matter component implies $\Omega_\chi h_0^2 \approx 0.17$ which is reachable in this model for $m_\chi \gtrsim 100$ GeV.

It is interesting to note that values of $\Omega_\chi h_0^2 \lesssim 0.25$

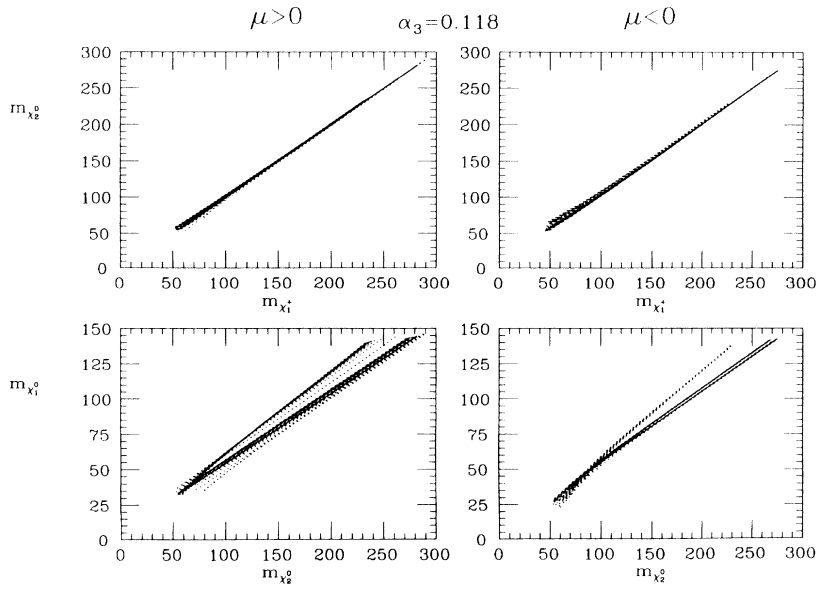

FIG. 5. Scatter plots of the second-to-lightest neutralino (χ_2^0) mass vs the lightest chargino ($\chi_1^\pm$) mass and second-to-lightest (χ_2^0) to lightest (χ_1^0) neutralino masses. Note the accuracy of the $m_{\chi_2^0} = m_{\chi_1^\pm}$ relation.

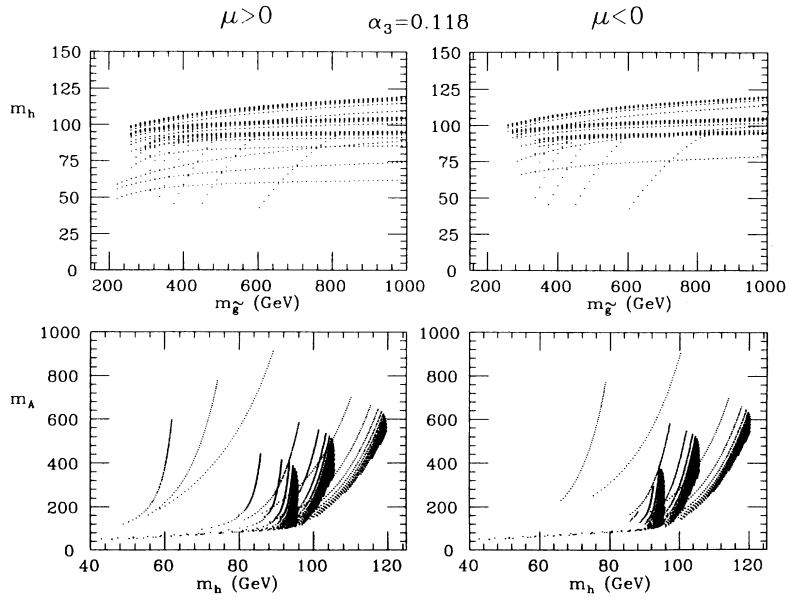

FIG. 6. Scatter plots of the one-loop corrected lightest Higgs boson mass m_h vs the gluino mass for $m_t = 100$, 130, and 160 GeV (top row), and the pseudoscalar Higgs mass m_A vs m_h (bottom row). The three noticeable bands (from bottom-to-top in the top row and from left-to-right in the bottom row) correspond to $m_t = 100$, 130, and 160 GeV. Note that in this model $m_A > m_h$ always. The heavy Higgs boson masses m_H and m_{H^+} are approached quickly from below by m_A.

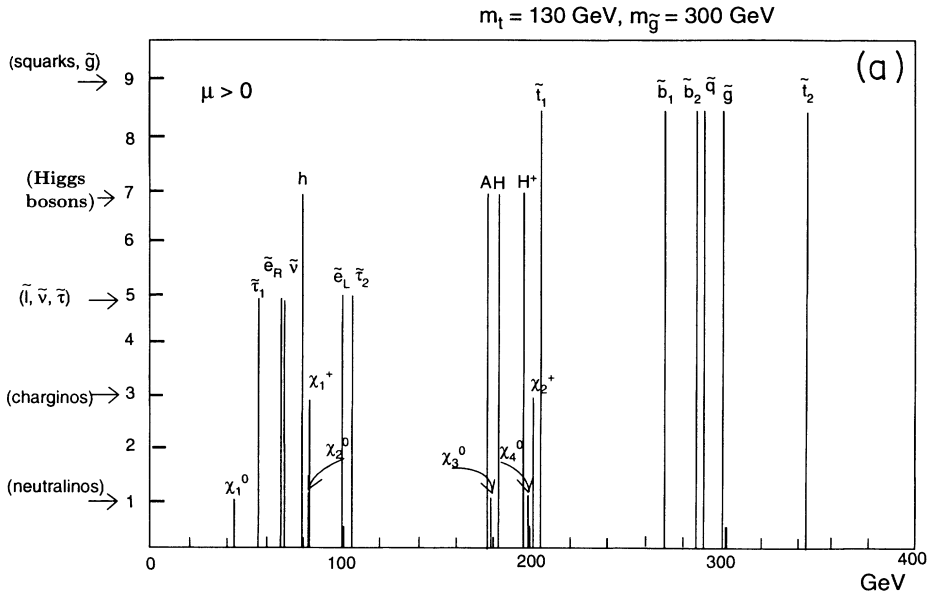

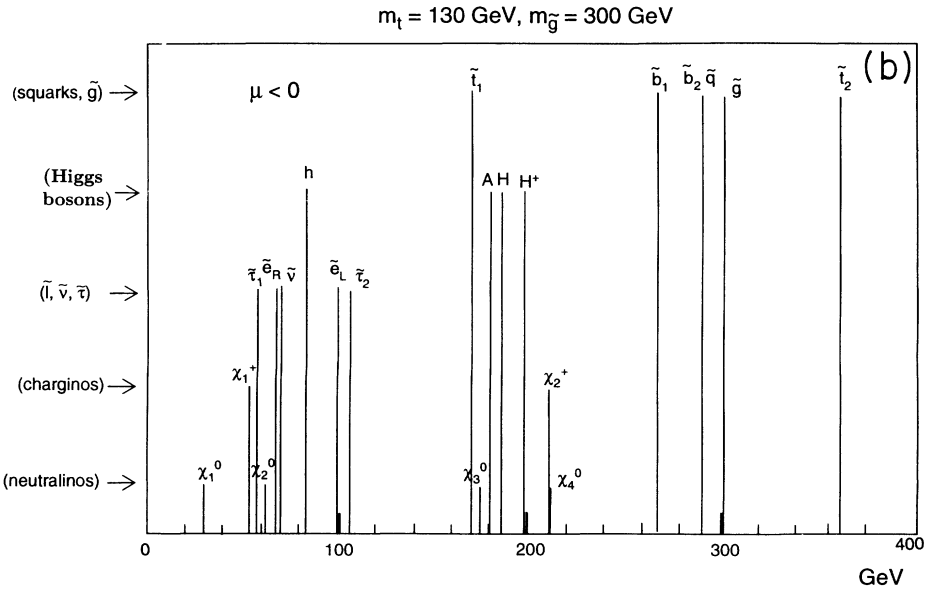

FIG. 7. Central values for the sparticle and one-loop corrected Higgs boson masses for $m_{\tilde{g}} = 300$ GeV, $m_t = 130$ GeV, $\alpha_3(M_Z) = 0.118$, and (a) $\mu > 0$ (b) $\mu < 0$. The masses generally scale with $m_{\tilde{g}}$. The percentage deviations from the shown values due to the variations in $\tan\beta$ are given in Table III.

TABLE III. Central values of the sparticle and one-loop corrected Higgs boson masses for $\alpha_3(M_Z)=0.118$, $m_{\tilde{g}}=300$ GeV, $m_t=130$ GeV, and both signs for μ, showing the percentage deviations from the central value due to the variation of $\tan\beta$ over its whole allowed range ($2 \lesssim \tan\beta \lesssim 32$).

i	$\tilde{m}_i(\mu>0)$	(%)	$\tilde{m}_i(\mu<0)$	(%)
μ	164	17	−164	17
$\tilde{q}$	290	0.1	290	0.1
χ_1^0	43	8.9	29	18
χ_2^0	83	19	62	2.1
χ_3^0	178	12	174	12
χ_4^0	197	11	212	13
$\chi_1^\pm$	83	20	53	9.3
$\chi_2^\pm$	201	8.2	210	11
h	79	23	82	19
H	183	35	185	32
A	177	32	179	30
H^+	195	26	198	24
$\tilde{e}_L$	100	2.2	100	2.2
$\tilde{e}_R$	68	4.2	68	4.2
$\tilde{\nu}$	69	8.5	69	8.5
$\tilde{\tau}_1$	56	21	57	18
$\tilde{\tau}_2$	105	7.3	105	6.8
$\tilde{b}_1$	270	3.5	267	3.2
$\tilde{b}_2$	286	0.5	290	1.0
$\tilde{t}_1$	205	8.2	170	7.8
$\tilde{t}_2$	344	3.4	363	1.3

occur naturally in this model, and in general for $m_{1/2} \gg m_0$. This situation is in sharp contrast to, for example, the minimal SU(5) supergravity model, where $\Omega_\chi h_0^2 \gg 1$ occurs naturally instead [23].

IV. THE STRICT NO-SCALE CASE

We now impose the additional constraint on the theory that $B(M_U)=0$, that is the strict no-scale case. Since $B(M_Z)$ is determined by the radiative electroweak symmetry breaking conditions, this added constraint needs to be imposed in a rather indirect way. That is, for given $m_{\tilde{g}}$ and m_t values, we scan the possible values of $\tan\beta$ looking for cases where $B(M_U)=0$. The most striking result is that solutions exist *only* for $m_t \lesssim 135$ GeV if $\mu>0$ and for $m_t \gtrsim 140$ GeV if $\mu<0$. That is, the value of m_t *determines* the sign of μ. Furthermore, for $\mu<0$ the value of $\tan\beta$ is determined uniquely as a function of m_t and $m_{\tilde{g}}$, whereas for $\mu>0$, $\tan\beta$ can be double valued for some m_t range which includes $m_t=130$ GeV but does not include $m_t=100$ GeV. In Fig. 8 (top row) we plot the solutions found in this manner for the indicated m_t values.

All the mass relationships deduced in the previous section apply here as well. The $\tan\beta$-spread that some of them have will be much reduced though. The most noticeable changes occur for the quantities which depend most sensitively on $\tan\beta$, i.e., the neutralino relic abundance and the lightest and pseudoscalar Higgs masses. In Fig. 8 (bottom row) we plot $\Omega_\chi h_0^2$ versus m_χ for this case. Note that continuous values of m_t will tend to fill in the space between the lines shown. In Fig. 9 (top row) we plot the one-loop corrected lightest Higgs boson mass versus $m_{\tilde{g}}$. The result is that m_h is basically determined by m_t; only a weak dependence on $m_{\tilde{g}}$ exists. Moreover, for $m_t \lesssim 135$ GeV $\Longrightarrow \mu>0, m_h \lesssim 105$ GeV; whereas for $m_t \gtrsim 140$ GeV $\Longrightarrow \mu<0, m_h \gtrsim 100$ GeV. Therefore, in the strict no-scale case, once the top-quark mass is measured, we will know the sign of μ and whether m_h is above or below 100 GeV. The pseudoscalar Higgs mass dependence on m_h is also much simplified, as Fig. 9 (bottom row) shows.

For $\mu>0$, we just showed that the strict no-scale constraint requires $m_t \lesssim 135$ GeV. This implies that μ cannot grow as large as it did previously. In fact, for $\mu>0$, $\mu_{\max} \approx 745$ GeV before and $\mu_{\max} \approx 440$ GeV now. This

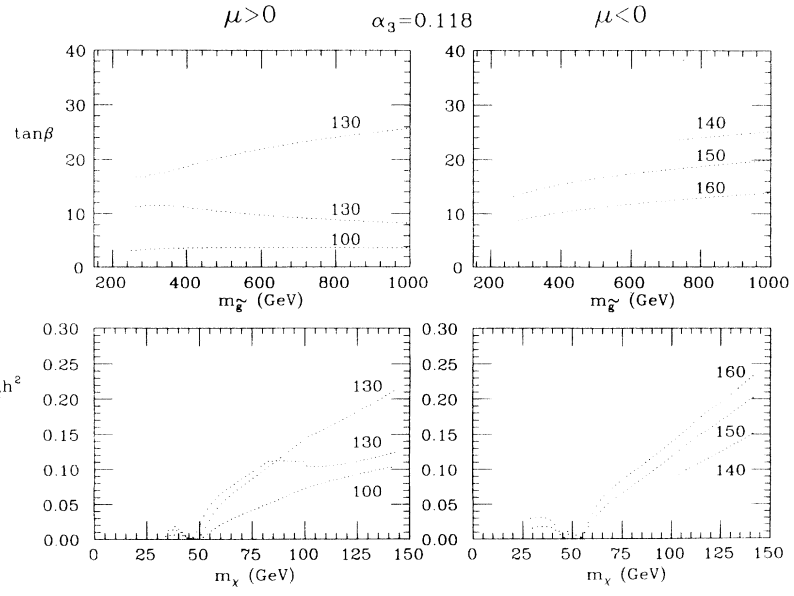

FIG. 8. Scatter plots of $\tan\beta$ vs $m_{\tilde{g}}$ for the strict no-scale case [where $B(M_U)=0$] for the indicated values of m_t. Note that the sign of μ is *determined* by m_t and that $\tan\beta$ can be double-valued for $\mu>0$. Also shown are the values of the neutralino relic abundance ($\Omega_\chi h_0^2$ vs m_χ) for the same values of the parameters.

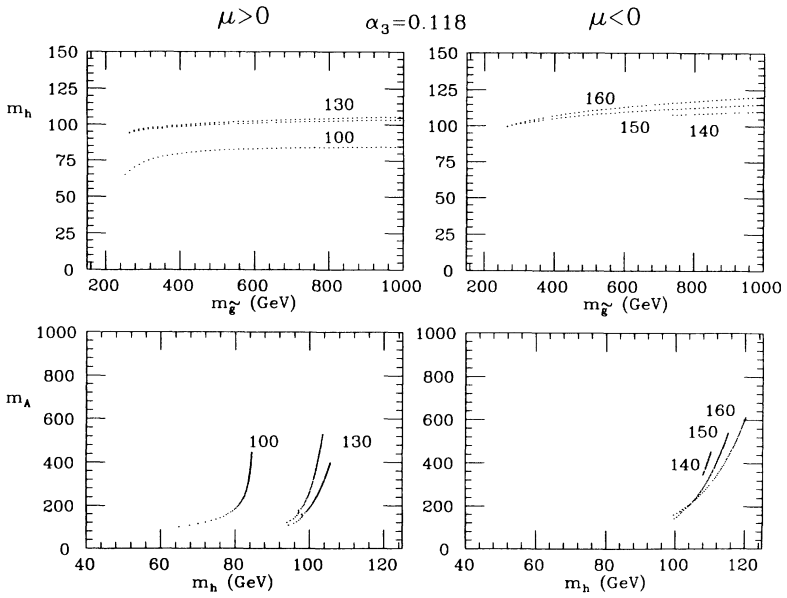

FIG. 9. Same as Fig. 6, but for the strict no-scale case. Note the weak dependence of m_h on the gluino mass $m_{\tilde{g}}$. Also, if $\mu>0$ for $m_t \lesssim 135$ GeV, $m_h \lesssim 105$ GeV; whereas if $\mu<0$, for $m_t \gtrsim 140$ GeV, $m_h \gtrsim 100$ GeV.

smaller value of $\mu_{\max}$ has the effect of cutting off the growth of the $\chi^0_{3,4}, \chi^{\pm}_2$ masses at $\approx\mu_{\max}\approx 440$ GeV (cf. ≈ 750 GeV) and of the heavy Higgs masses at ≈ 530 GeV (cf. ≈ 940 GeV).

V. CONCLUSIONS

In this paper we have presented the simplest, string-derivable, supergravity model and deduced its experimental predictions. This new string-inspired model has several features that are found in real string-derived models, such as string unification and a unified gauge group which can reduce to the standard model one after spontaneous gauge symmetry breaking. We also demanded that the low-energy supergravity theory be of the no-scale type, since this general framework is supported by superstring theory. The model built this way should be considered to be an idealization of what its string-derived incarnation should be. In the process we have identified several potential model-building problems which would need to be watched for in a string implementation. We have assumed that the various needed mass scales are generated somehow and have fit their values to achieve string unification at $M_U = 10^{18}$ GeV. The actual origin of these mass scales will lie within the structure of the successful string model. Known examples include condensates [11,32] and vacuum expectation values [33] of hidden matter fields. As in any nonminimal flipped SU(5) model, non-negligible dimension-five proton decay operators could be reintroduced. In the model presented here these remain highly suppressed. However, in variants of this model or in string-derived versions, these operators could exist at an observable level. This question deserves further study.

We have also performed a thorough and accurate exploration of the parameter space of the model and solved for all the sparticle and one-loop corrected Higgs masses. The growth of the supersymmetry breaking parameter is cut off by the no-scale supergravity mechanism which guarantees $m_{\tilde{q}}, m_{\tilde{g}} < 1$ TeV. We found some general results and upper bounds on the sleptons and lightest neutralino, chargino, and Higgs masses. We have also found several simple relations among squark and gluino masses, among slepton masses, and among the lightest neutralino and chargino masses. The neutralino relic abundance $\Omega_\chi h_0^2$ never exceeds ≈ 0.25 and therefore does not constrain this model. However, it may constitute a significant portion of the dark matter in the Universe in general and in the galactic halo in particular. In the strict no-scale case we find a striking result: if $\mu>0$, $m_t \lesssim 135$ GeV, whereas if $\mu<0$, $m_t \gtrsim 140$ GeV. Therefore the value of m_t determines the sign of μ. Moreover, the value of $\tan\beta$ can also be determined. Furthermore, we found that the value of m_t also determines whether the lightest Higgs boson is above or below 100 GeV.

ACKNOWLEDGMENTS

This work has been supported in part by DOE Grant No. DE-FG05-91-ER-40633. The work of J. L. has been supported by the SSC Laboratory. The work of D.V.N. has been supported in part by a grant from Conoco Inc. We would like to thank the HARC Supercomputer Center for the use of their NEC SX-3 supercomputer.

[1] S. Barr, Phys. Lett. **112B**, 219 (1982); Phys. Rev. D **40**, 2457 (1989); J. Derendinger, J. Kim, and D. V. Nanopoulos, Phys. Lett. **139B**, 170 (1984).

[2] I. Antoniadis, J. Ellis, J. Hagelin, and D. V. Nanopoulos, Phys. Lett. B **194**, 231 (1987).

[3] I. Antoniadis, J. Ellis, J. Hagelin, and D. V. Nanopoulos, Phys. Lett. B **231**, 65 (1989).

[4] J. Ellis, J. Hagelin, S. Kelley, and D. V. Nanopoulos,

Nucl. Phys. **B311**, 1 (1988/89).
[5] I. Antoniadis, J. Ellis, R. Lacaze, and D. V. Nanopoulos, Phys. Lett. B **268**, 188 (1991); S. Kalara, J. L. Lopez, and D. V. Nanopoulos, *ibid.* **269**, 84 (1991).
[6] J. Ellis, S. Kelley, and D. V. Nanopoulos, Phys. Lett. B **249**, 441 (1990); F. Anselmo, L. Cifarelli, and A. Zichichi, Nuovo Cimento **105A**, 1335 (1992).
[7] I. Antoniadis, J. Ellis, S. Kelley, and D. V. Nanopoulos, Phys. Lett. B **272**, 31 (1991); D. Bailin and A. Love, *ibid.* **280**, 26 (1992).
[8] S. Kelley, J. L. Lopez, and D. V. Nanopoulos, Phys. Lett. B **278**, 140 (1992); G. Leontaris, *ibid.* **281**, 54 (1992).
[9] For a review see, e.g., J. L. Lopez and D. V. Nanopoulos, in *Proceedings of the 15th Johns Hopkins Workshop on Current Problems in Particle Theory,* Baltimore, Maryland, 1991, edited by G. Domokos and S. Kovesi-Domokos (World Scientific, Singapore, 1992), p. 277.
[10] J. Ellis, S. Kelley, and D. V. Nanopoulos, Phys. Lett. B **260**, 131 (1991).
[11] J. L. Lopez and D. V. Nanopoulos, Phys. Lett. B **251**, 73 (1990); **256**, 150 (1991); **268**, 359 (1991).
[12] For a review see A. B. Lahanas and D. V. Nanopoulos, Phys. Rep. **145**, 1 (1987).
[13] E. Witten, Phys. Lett. **155B**, 151 (1985).
[14] J. Ellis, C. Kounnas, and D. V. Nanopoulos, Nucl. Phys. **B241**, 406 (1984).
[15] J. Ellis, C. Kounnas, and D. V. Nanopoulos, Nucl. Phys. **B247**, 373 (1984).
[16] J. Ellis, A. Lahanas, D. V. Nanopoulos, and K. Tamvakis, Phys. Lett. **134B**, 429 (1984).
[17] S. Kelley, J. L. Lopez, D. V. Nanopoulos, H. Pois, and K. Yuan, Phys. Lett. B **273**, 473 (1991).
[18] S. Kalara, J. Lopez, and D. V. Nanopoulos, Phys. Lett. B **245**, 421 (1990); Nucl. Phys. **B353**, 650 (1991).
[19] S. Kelley, J. L. Lopez, and D. V. Nanopoulos, Phys. Lett. B **261**, 424 (1991).
[20] J. Ellis, J. L. Lopez, and D. V. Nanopoulos, Phys. Lett. B **292**, 189 (1992).
[21] J. L. Lopez, D. V. Nanopoulos, and K. Yuan, Nucl. Phys. **B399**, 654 (1993).
[22] M. Matsumoto, J. Arafune, H. Tanaka, and K. Shiraishi, Phys. Rev. D **46**, 3966 (1992); R. Arnowitt and P. Nath, Phys. Rev. Lett. **69**, 725 (1992); J. Hisano, H. Murayama, and T. Yanagida, *ibid.* **69**, 1014 (1992); Nucl. Phys. **B402**, 46 (1993).
[23] J. L. Lopez, D. V. Nanopoulos, and A. Zichichi, Phys. Lett. B **291**, 255 (1992); J. L. Lopez, D. V. Nanopoulos, and H. Pois, Phys. Rev. D **47**, 2468 (1993).
[24] S. Bethke, in *Proceedings of the XXVIth International Conference on High Energy Physics,* Dallas, Texas, 1992, edited by J. R. Sanford, AIP Conf. Proc. No. 272 (AIP, New York, 1993), p. 81.
[25] S. Kelley, J. L. Lopez, D. V. Nanopoulos, H. Pois, and K. Yuan, Nucl. Phys. **B398**, 3 (1993).
[26] P. Nath and R. Arnowitt, Phys. Lett. B **289**, 368 (1992).
[27] M. Drees and M. M. Nojiri, Phys. Rev. D **45**, 2482 (1992).
[28] S. Kelley, J. L. Lopez, D. V. Nanopoulos, H. Pois, and K. Yuan, Phys. Lett. B **285**, 61 (1992).
[29] J. L. Lopez, D. V. Nanopoulos, and K. Yuan, Nucl. Phys. **B370**, 445 (1992); Phys. Lett. B **267**, 219 (1991); S. Kelley, J. L. Lopez, D. V. Nanopoulos, H. Pois, and K. Yuan, Phys. Rev. D **47**, 2461 (1993).
[30] See, e.g., E. Kolb and M. Turner, *The Early Universe* (Addison-Wesley, Reading, MA, 1990).
[31] See, e.g., R. Schaefer and Q. Shafi, Nature (London) **359**, 199 (1992); A. N. Taylor and M. Rowan-Robinson, *ibid.* **359**, 393 (1992).
[32] S. Kalara, J. L. Lopez, and D. V. Nanopoulos, Phys. Lett. B **275**, 304 (1992).
[33] I. Antoniadis, J. Rizos, and K. Tamvakis, Phys. Lett. B **278**, 257 (1992).